5.3. DESIGN EXAMPLES

As was mentioned earlier, channels can either be classified as wide or narrow. The design procedure for each case will be slightly different. This is because for wide channels, $\delta_{cr}^* = d_{cr\max}^*$ for the given value of μ, while for narrow channels, δ_{cr}^* is initially unknown and must therefore be determined by trial and error. Four examples will be used to demonstrate how each type of channel is designed using the equations and graphs that have been developed here.

5.3.1. WIDE CHANNEL; SLOPE GIVEN

A channel is to be composed of semi-angular material with $\mu = 0.76$, $d_{90} = 80$ mm, and $d_{50} = 60$ mm. It is to have a slope $S = 0.0016$ and required to support a discharge $Q = 350$ m^3/s. Assuming lift-to-drag ratio $\beta = 0.85$ and dimensionless critical shear stress $\tau_{cr}^* = 0.03$, determine the dimensions and bank shape of the channel.

1) Assuming this is a wide channel, from Figure 5.7, $\delta_{cr}^* = 0.897$. Using Equation 20, $D_c =$ 2.07 m.
2) Using Figure 5.5e, $B_s^* = 5.76$. This means $B_s = B_s^* D_c =$ 11.92 m.
3) Figure 5.14e gives $Q_{bank}^* = 9.14$; $Q_{bank} = 37.00$ m^3/s.
   $Q_f = Q - Q_{bank} = 313.00$ m^3/s.
   Assume that $B_f^* = 5.0$, the minimum for a wide channel. Substituting this in Equation 40, $Q_f = 52.9$ m^3/s. Since this is less than the required value of 313.00 m^3/s, B_f^* is greater than 5.0, and the assumption that the channel is wide is correct. Solving equation 40 by trial and error, $B_f^* = 28.8$. Therefore, $B_f = B_f^* D_c =$ 59.62 m.
4) The top channel width $B = D_c\left(B_f^* + B_s^*\right) =$ 71.54 m.
5) The wide channel's bank profile is generated using the equation $D^* = -0.009d^{*3} - 0.0701d^{*2} - 0.0662d^* + 1.0018$, the coefficients of which are taken from Table 5.5.

To complete the design process, the rate of bedload transport needs to be determined. In reality, the design engineer has to select a bedload relation that is suitable to his particular case. There are numerous sediment transport relations from which to choose; e.g., the equations proposed by Engelund and Hansen (1967), Ashida and Michiue (1972), and Parker (1979). However, for the design examples discussed here, the Ashida-Michiue sediment transport equation is arbitrarily used.

$$q_B = 17\sqrt{R_s g d_{50}^*}\, t_{ave}^* \left(1 - \frac{t_{cr}^*}{t_{ave}^*}\right)\left(1 - \sqrt{\frac{t_{cr}^*}{t_{ave}^*}}\right) \qquad (43a)$$

where

q_B = volumetric bedload transport per unit width

t_{ave}^* = average dimensionless shear stress over the flat-bed region

The value for t_{ave}^* can be determined by using the following equation:

$$t^*_{ave} = \left[1 + \frac{2\left(d^*_{cr} - 1\right)\sqrt{y_0}}{B^*_f} \tanh\left(\frac{B^*_f}{2\sqrt{y_0}}\right)\right]\left(\frac{t^*_{cr}}{d^*_{cr}}\right) \quad (43b)$$

The derivation of Equation 43b can be found in Appendix D. Equation 43b gives a value of 0.0333 for t^*_{ave}. Substituting this in equation 43a yields a bedload transport rate of 3.02E-5 m^2/s. Since bedload transport is assumed to occur over the entire width of the flat-bed region, the total bedload transport rate $Q_s = q_B B_f$ = 1.80E-3 m^3/s.

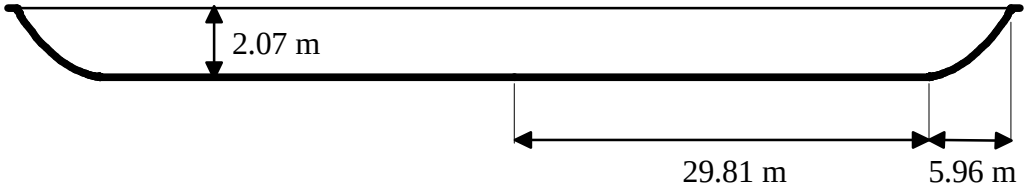

Figure 5.16a. Wide channel designed using graphical method; slope given

The wide channel designed using the graphical method is shown in Figure 5.16a. As a basis for comparison, a channel with a flat bed and cosine banks, will be designed for the same conditions. This is referred to as a Type A channel, and is often used in channel design. The following equations found in Henderson (1966) will be used for this purpose.

$$D_c = \frac{d_{50}}{20.2S}\text{; } d_{50} \text{ is in meters} \quad (44)$$

$$B_s = \frac{pD_c}{\tan f} \quad (45)$$

$$A_{bank} = \frac{2D_c^2}{\tan f} \quad (46)$$

$$P_{bank} = \frac{2D_c E}{\sin f} \text{ = wetted perimeter of bank region} \quad (47)$$

where

ϕ = angle of repose; $\tan\phi = \mu$

P_{bank} = wetted perimeter of bank region

$$E = \frac{p}{2}\left(1 - \tfrac{1}{4}\sin^2 f\right)$$

For this case, $\phi = 37.2^o$. Equations 44 to 47 yield D_c = 1.86 m, , B_s = 7.67 m, A_{bank} = 9.07 m^2, and P_{bank} = 8.76 m, respectively. Manning's equation will be used to determine the flat-bed width B_f of the channel.

$$Q = \frac{A^{\frac{5}{3}} S^{\frac{1}{2}}}{nP^{\frac{2}{3}}} \quad (48)$$

where

n = roughness coefficient = $\frac{d_{50}^{\frac{1}{6}}}{21.1}$; d_{50} is in meters (49)

A = cross-sectional area of channel = $A_{bank} + B_f D_c$ (50)

P = wetted perimeter of channel = $P_{bank} + B_f$ (51)

Equation 49 gives a roughness coefficient of 0.0297. All terms in Equations 50 and 51 are now known except for B_f. Substituting these in Equation 48, and noting that the channel discharge is 600 m^3/s, results in the following expression:

$$350 = \frac{\left(9.07 + 1.86B_f\right)^{\frac{5}{3}}(0.0016)^{\frac{1}{2}}}{0.0297\left(8.76 + B_f\right)^{\frac{2}{3}}} \quad (52)$$

Solving this equation by trial and error, B_f = 90.00 m. Therefore, the channel's top channel width $B = B_s + B_f$ = 97.67 m.

The optimal stable channel is slightly deeper and has a significantly wider bank region than the Type A channel. Examination of the D_c and B_s values of both channels shows that the cosine banks are steeper. Since all particles on the banks of the optimal stable channel are on the verge of motion, this implies that the cosine banks are unstable. The optimal channel design also predicts a top channel width that is much narrower than that resulting from the second design. This implies that the optimal stable channel requires a smaller cross-sectional area than the Type A channel, to accommodate a given water discharge. One more thing to note is that the design of the Type A channel is based on the assumption that the channel only conveys water. Thus, its design does not involve any clear method of accounting for bedload motion.

5.3.2. NARROW CHANNEL; SLOPE GIVEN

A channel is to be composed of material with $\mu = 0.76$, $d_{90} = 80$ mm, and $d_{50} = 60$ mm. It is to have a slope S = 0.0016 and required to support a discharge Q = 50 m^3/s. Assume lift-to-drag ratio $\beta = 0.85$ and dimensionless critical shear stress $\tau_{cr}^* = 0.03$, determine the dimensions and bank shape of the channel.

1) Assume $\delta_{cr}^* = 0.897$. Using Equation 20, D_c = 2.07 m.
2) Using Figure 5.5e, $B_s^* = 5.76$. This means $B_s = B_s^* D_c$ = 11.92 m.
3) Figure 5.14e gives $Q_{bank}^* = 9.14$; Q_{bank} = 37.00 m^3/s.
   $Q_f = Q - Q_{bank}$ = 13.00 m^3/s.

   Assume that $B_f^* = 5.0$. Using equation 40, Q_f = 52.92 m^3/s. Since this is greater than 13.00 m^3/s, B_f^* is less than 5.0. The channel is therefore narrow, but the assumed value for δ_{cr}^* is incorrect. A smaller value for δ_{cr}^* must be assumed.

   By trial, when $\delta_{cr}^* = 0.882$, D_c = 2.1 m, B_s = 12.54 m, Q_{bank} = 40.22 m^3/s, and Q_f = 9.78 m^3/s. The B_f^* value which corresponds to $\delta_{cr}^* = 0.882$ is determined using Figure 5.6e; $B_f^* = 0.90$. Using this in equation 40, Q_f = 9.78 m^3/s. Since the two

Q_f values match, the assumed value for δ_{cr}^*, and the corresponding value for B_f^* are correct. Therefore, D_c = 2.1 m, B_s = 12.54 m, and $B_f = B_f^* D_c$ = 1.89 m.

4) The top channel width $B = D_c\left(B_f^* + B_s^*\right)$ = 14.43 m.
5) The narrow channel's bank profile is generated using the equation $D^* = -0.00998y^{*3} - 0.06204y^{*2} - 0.0549y^* + 1.00146$, whose coefficients are interpolated from the values found in Table 5.5. Figure 5.16b shows the designed narrow channel.

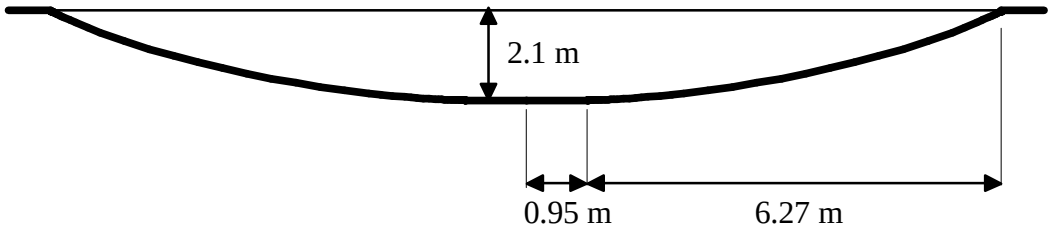

Figure 5.16b. Narrow channel designed using graphical method; slope given

Equation 43b gives a value of 0.0304 for t_{ave}^*. Using this in equation 43a, the bedload discharge is computed; q_B = 5.3E-7 m^2/s and thus Q_s = 1.0E-6 m^3/s.

A channel with cosine banks is again designed for the purposes of comparison. All conditions for this case are the same as those for the wide channel case except for channel discharge which is now 50 m^3/s. Therefore, the following are still the same: D_c = 1.86 m, B_s = 7.67 m, A_{bank} = 9.07 m, P_{bank} = 8.76 m, and n = 0.0297. Substituting Equations 50 and 51 in Equation 48, and noting that Q = 50 m^3/s, results in the following equation:

$$50 = \frac{\left(9.07 + 1.86B_f\right)^{\frac{5}{3}}(0.0016)^{\frac{1}{2}}}{0.0297\left(8.76 + B_f\right)^{\frac{2}{3}}} \qquad (53)$$

By trial and error, B_f = 10.47 m. B = 7.67 + 10.47 = 18.14 m. Comparison of these two channels again shows the optimal stable channel to have a slightly greater center depth, a significantly wider bank region, and a much narrower top width. This implies that for the narrow channel case, the optimal stable channel still has gentler banks, and requires a smaller cross-sectional area to convey a given discharge.

The preceding examples are based on the assumption that slope S is given and bedload discharge Q_s is a dependent variable. In stable channel design, it is also possible to have Q_s as a given and S as a dependent variable. For such a case, the design approach will vary, depending on the sediment transport relation that is used. The considerable number of sediment transport equations available makes it impractical to discuss every design variation. Therefore, only two examples will be presented, with the Ashida-Michiue formula again used for this purpose.

5.3.3. WIDE CHANNEL; SEDIMENT DISCHARGE RATE GIVEN

A channel is to be composed of semi-angular material with μ = 0.84, d_{90} = 75 mm, and d_{50} = 45 mm. It is required to support a water discharge Q = 600 m^3/s and a sediment discharge Q_s = 1.57E-3 m^3/s. Assuming β = 0.85 and τ^*_{cr} = 0.03, determine the dimensions and bank shape of the channel.

1) Assuming this is a wide channel, from Figure 5.7, δ^*_{cr} = 0.89. Moreover, assume that D_c = 4.0 m. Equation 20 yields a value of slope S = 0.000626.
2) Using Figure 5.5f, B^*_s = 5.42. This means $B_s = B^*_s D_c$ = <u>21.68 m</u>.
3) Using Figure 5.14f, Q_{bank} = 129.4 m^3/s. $Q_f = Q - Q_{bank}$ = 470.6 m^3/s. Solving Equation 40 by trial and error, B^*_f = 11.94. $B_f = B^*_f D_c$ = <u>47.76 m</u>.
4) Using Equations 43b and 43a respectively, t^*_{ave} = 0.033 and q_B = 1.91E-5 m^2/s. $Q_s = q_B B_f$ = 9.12E-4 m3/s.

   Since this is different from the given Q_s value, the assumed value for D_c is incorrect. A new value for D_c must be assumed and steps 1 to 4 repeated until the correct value has been found.

   When D_c is assumed to be 3.09 m, S =0.00081, B_s = 16.75 m, Q_{bank} = 74.0 m^3/s, Q_{bed} = 526.0 m^3/s, B^*_f = 23.15, B_f = 71.53 m, t^*_{ave} = 0.0335, q_B = 2.2E-5 m^2/s, and Q_s = 1.56E-3 m^3/s. Since this matches the given value of Q_s, the assumed value for D_c is correct. Therefore D_c = <u>3.09 m</u>, B_s = <u>16.75 m</u>, and B_f = <u>71.53 m</u>.
5) The top channel width $B = D_c\left(B^*_f + B^*_s\right)$ = <u>88.28 m</u>.
6) The wide channel's bank profile is generated using the equation $D^* = -0.013d^{*3} - 0.0708d^{*2} - 0.0742d^* + 1.0021$, the coefficients of which are taken from Table 5.5. Figure 5.17a shows the designed wide channel.

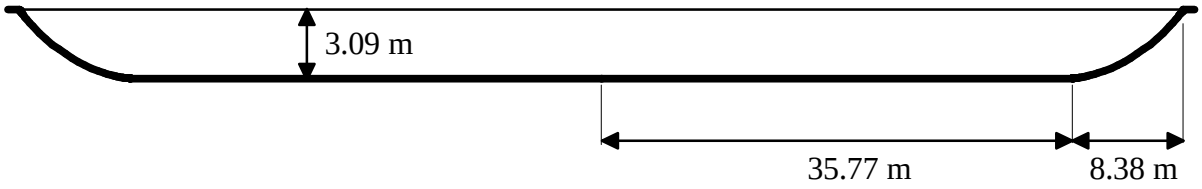

Figure 5.17a. Wide channel designed using graphical method; sediment discharge rate given

5.3.4. NARROW CHANNEL; SEDIMENT DISCHARGE RATE GIVEN

A channel is to be composed of material with μ = 0.84, d_{90} = 75 mm, and d_{50} = 45 mm. It is required to support a water discharge Q = 132 m^3/s and a sediment discharge Q_s = 4.62E-5 m^3/s. Assume lift-to-drag ratio β = 0.85 and dimensionless critical shar stress τ^*_{cr} = 0.03, determine the dimensions and bank shape of the channel.

1) Assume that δ^*_{cr} = 0.886. Using Figure 5.6f, B^*_f = 2.14.
2) Assume that D_c = 4.0 m. Using Equation 43b results in t^*_{ave} = 0.0314.

3) Equation 43a yields a value of 3.60E-6 for q_B. $Q_s = q_B B_f D_c$ = 3.08E-5 m^3/s. Since this is different from the given Q_s value, the assumed value for D_c is incorrect. A new value for D_c must be assumed and steps 2 and 3 repeated until the value of D_c is such that it leads to the given value of Q_s.

   When D_c is assumed to be 6.43 m, t^*_{ave} = 0.0313, q_B = 3.36E-6 m^2/s, and Q_s 4.62E-5 m3/s. Since this matches the given value of Q_s, the assumed value for D_c can be used to determine S.

4) Using equation 20, S = 0.00039.
5) Using Figure 5.5f, B^*_s = 5.48.
6) Using Figure 5.14f, Q_{bank} = 366.9 m^3/s. Even without adding Q_{bed}, this already exceeds the total water discharge which is only 132 m^3/s. The assumed value for δ^*_{cr} is therefore incorrect. A new value for δ^*_{cr} must be assumed and steps 1 to 6 repeated until the given value of Q_s is obtained.

   When δ^*_{cr} = 0.888, B^*_f =2.66, D_c = 3.097 m (again found by trial and error), S = 0.00081, B^*_s = 5.46, Q_{bank} = 74.75 m^3/s, Q_{bed} = 57.23 m^3/s, Q = 132.0 m^3/s, t^*_{ave} = 0.0335, q_B = 5.61E-6 m^2/s, and Q_s = 4.62E-5 m^3/s. Since the calculated values of Q and Q_s, match their respective given values, the assumed value for δ^*_{cr} is correct. Therefore, D_c = <u>3.097 m</u>, $B_s = B^*_s D_c$ = <u>16.92 m</u>, and $B_f = B^*_f D_c$ = <u>8.24 m</u>.

7) The top channel width $B = D_c\left(B^*_f + B^*_s\right)$ = <u>25.16 m</u>.
8) The narrow channel's bank profile is generated using the equation $D^* = -0.0132y^{*3} - 0.0693y^{*2} - 0.0733y^* + 1.00208$, whose coefficients are interpolated from the values found in Table 5.5. Figure 5.17b shows the designed narrow channel.

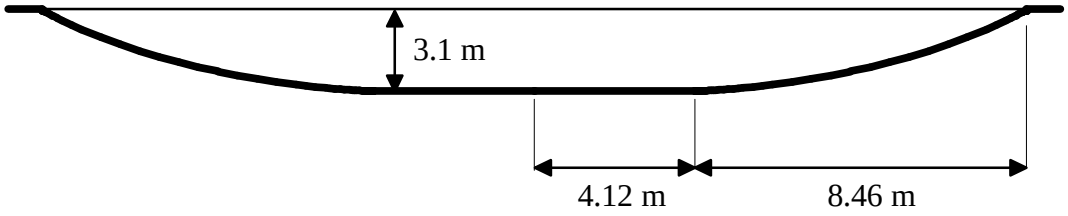

Figure 5.17b. Narrow channel designed using graphical method; sediment discharge rate given

5.4. MODEL VERIFICATION

Experimental and field data are used to verify the results of the numerical model. Data provided by Ikeda (1981), Ikeda et. al. (1988), and Diplas (1990), were obtained from laboratory experiments on self-formed stable channels. Ikeda used a glass flume 15 m long and 0.5 m wide. A well graded sand with median diameter d_{50} = 1.3 mm and gradation coefficient σ_g = 1.3 was used in his experiments. Ikeda et. al. used a similar flume and quartz sand. Diplas used a 14.6 m long, 0.53 m wide flume, containing sand with median diameter d_{50} = 1.9 mm and standard deviation σ_g = 1.45. In selecting data from these three sources, it was necessary to make sure that

flows were deep enough to preclude any significant surface tension effects, and that the sediment was coarse enough to prevent its suspension. Furthermore, the channels considered must have reached equilibrium, i.e., their cross-sections should no longer experience any noticeable changes in size and shape. Tables 5.7a to 5.7c show the significant experimental data used in testing the numerical model.

Kellerhals (1967), Bray (1979) and Hey and Thorne (1987), gathered data from natural rivers. The data chosen from these three sources satisfy the following criteria set by Ikeda, Parker, and Kimura (1988): (1) mobile beds must be hydraulically rough, (2) bed material must be actively transported at flood stage, (3) the river or canal must be nearly straight, (4) water discharge Q, longitudinal slope S, and grain size information must be specified, and (5) vegetation should not have a material effect on the channel geometry. These data are found in Tables 5.8a to 5.8c.

The field data taken from Kellerhals, Bray, and Hey and Thorne yielded average critical Shields stress values of 0.023, 0.04, and 0.033, respectively. The experimental data, on the other hand, yielded higher values of τ_{cr}^{*}. These were 0.035, 0.048, and 0.056 for Ikeda, Ikeda et. al., and Diplas, respectively. The aforementioned values were used in calculating channel center depths. Figure 5.18 shows the values of center depth D_c predicted by the model, plotted against the corresponding measured values. These appear to be in good agreement.

Table 5.7a. Experimental data used to test numerical model; Ikeda (1981).

Run No.	Q (cm^3/sec)	mean D (cm)	B (cm)	S
15	7600	3.43	62.0	0.00214
16	8140	3.54	64.4	0.00209
17	8260	3.59	64.8	0.00216
18	8960	3.61	70.4	0.00198
19	9100	3.74	67.4	0.00182
20	9260	3.73	71.4	0.00201
21	9360	3.43	75.0	0.00222
22	9560	3.79	70.8	0.00199
23	9640	3.39	75.2	0.00230
24	9740	3.76	71.6	0.00190
25	9880	3.61	75.0	0.00216
26	9960	3.55	78.2	0.00214
27	10260	3.61	78.0	0.00202
28	10580	3.7	78.6	0.00202
29	10880	3.78	79.6	0.00203
30	11240	3.76	81.0	0.00207
31	11420	4.00	81.8	0.00196
32	11480	3.95	79.2	0.00196
33	11980	3.91	79.8	0.00197
34	12600	4.02	83.4	0.00199

Table 5.7b. Experimental data used to test numerical model; Ikeda, Parker, and Kimura (1988).

Run No.	Q (cm^3/sec)	D_c (cm)	B (cm)	S
B1	10000	4.70	66.6	0.00204
B2	8500	5.20	57.0	0.00196
B3	8380	5.40	54.0	0.00212
B4	10460	5.00	64.0	0.00222
B5	8960	4.80	60.2	0.00236
B6	8960	5.20	56.6	0.00213
B7	8720	5.05	57.2	0.00233
B8	6100	3.10	53.8	0.00340
B9	9460	5.70	57.6	0.00200
B10	9220	5.50	59.0	0.00223
C1	10740	5.60	66.2	0.00199
C3	6800	4.10	56.6	0.00261
C4	9380	4.00	70.4	0.00251
C5	5500	3.50	52.0	0.00330
C6	7100	3.65	61.2	0.00292
D1	9140	4.20	64.6	0.00337
D2	9220	3.60	69.8	0.00333
D3	9220	4.55	62.8	0.00295
D4	9240	3.90	69.0	0.00340
D5	8800	4.70	61.0	0.00267

Table 5.7c. Experimental data used to test numerical model, Diplas (1990).

	Q (cm^3/sec)	D_c (cm)	B (cm)	S
1	12526	4.90	65.8	0.0037
2	12920	4.52	70.8	0.0043
3	11246	3.60	79.6	0.0062
4	7826	3.50	59.0	0.0052
5	7800	3.10	64.0	0.0074
6	6520	2.82	58.8	0.0069

Table 5.8a. Field data used to test numerical model; Kellerhals (1967).

Sample	Q(m^3/sec)	D_c (m)	B (m)	S	d_{50} (mm)	d_{90} (mm)
2-1	42.48	1.067	22.251	0.0028	82.3	125.0
2-6	4.50	0.488	6.614	0.00295	42.7	57.9
2-12	3.62	0.445	6.675	0.00243	33.5	45.7
2-14	3.11	0.475	6.523	0.00139	20.1	25.0
2-15	13.51	0.762	12.009	0.00199	48.8	82.3
2-17	15.04	0.716	12.497	0.00274	36.6	48.8
3-3	229.94	3.109	24.689	0.00190	76.2	179.8

Table 5.8b. Field data used to test numerical model; Bray (1979).

Sequence No.	Q(m^3/sec)	D_c (m)	B (m)	S	d_{50} (mm)	d_{90} (mm)
1	6088.3	4.999	475.19	0.00074	46	81
2	7221.1	6.828	544.68	0.00069	41	81
7	453.1	1.737	114.91	0.003	60	132
8	906.2	2.585	191.11	0.00092	43	86
9	48.1	0.869	39.62	0.0054	42	78
16	481.4	2.381	94.79	0.0026	117	319
17	691.0	1.786	150.88	0.0025	63	127
19	85.0	0.981	40.23	0.0057	27	100
20	124.6	1.390	62.79	0.0012	27	49
22	169.9	1.219	71.63	0.0049	28	60
30	314.3	1.430	103.94	0.0020	33	56
31	438.9	1.701	125.58	0.0018	40	65
32	481.4	1.594	160.33	0.0012	26	72
33	750.4	2.420	165.51	0.00081	32	73
35	80.7	1.222	37.49	0.0058	30	60
36	23.8	0.710	26.21	0.0025	30	80
38	73.6	0.948	37.19	0.0059	37	75
47	283.2	1.582	109.73	0.0017	49	101
57	68.0	0.948	54.86	0.0019	30	51

Table 5.8c. Field data used to test numerical model; Hey and Thorne (1986).

Site No.	Q(m^3/sec)	D_c (m)	B (m)	S	d_{50} (mm)	d_{90} (mm)
23	7.1	0.50	13.7	0.006106	48.3	65.5
31	7.5	0.59	12.6	0.003429	86.0	118.4
36	11.2	0.87	14.1	0.005527	74.1	113.8
38	237.0	2.69	57.8	0.001455	55.7	73.4
53	358.3	2.05	77.1	0.001641	60.2	80.0
60	20.0	0.65	17.5	0.003557	20.2	26.6

Figure 5.19 is a comparison of predicted and observed values of top channel width B. It can be seen here that the model also predicts B well. In most cases, use of the model resulted in slight underpredictions of B. The only data source for which there was a consistent overprediction of B was that of Kellerhals. However, these discrepancies are also slight; the agreement between the predicted and observed values of B is still good.

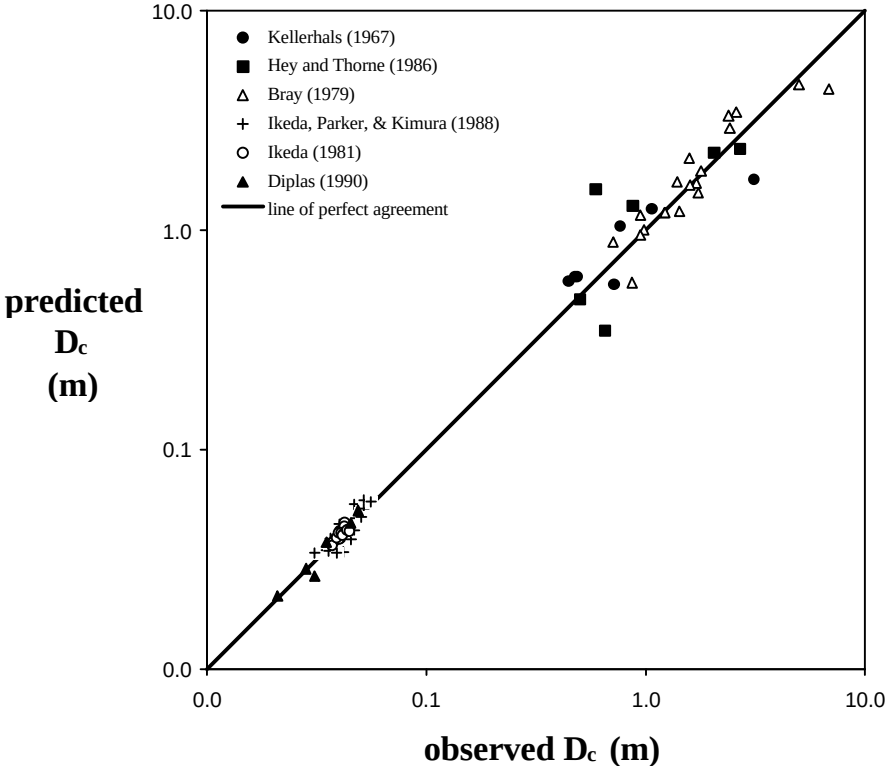

Figure 5.18. Comparison of observed and predicted values of channel center depth D_c

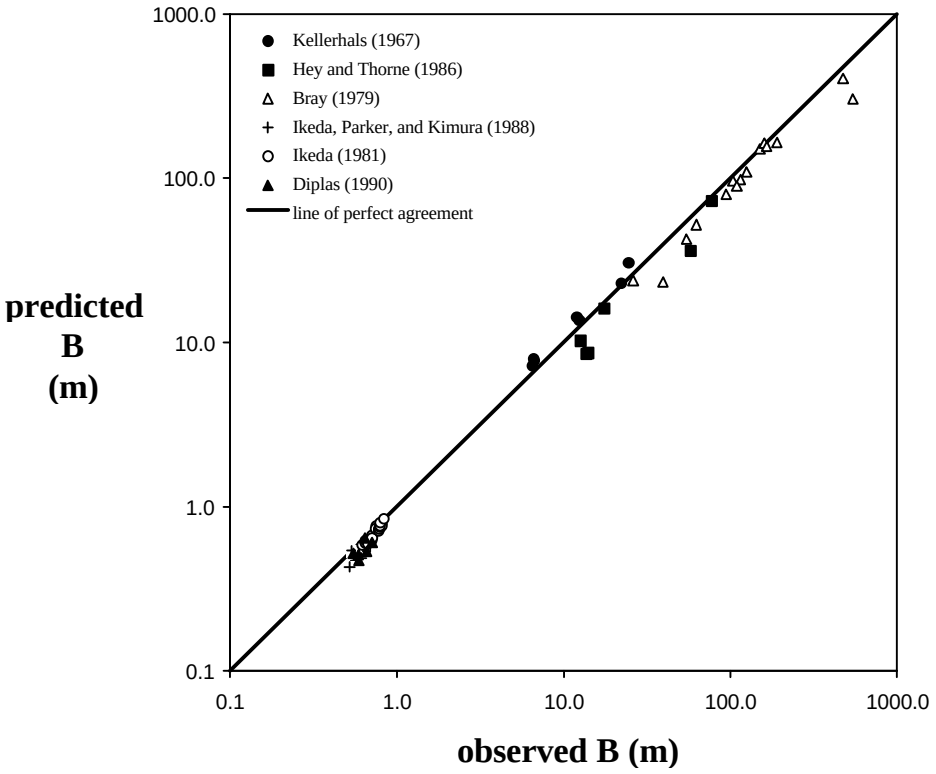

Figure 5.19. Comparison of observed and predicted values of top channel width B

5.5 LIMITATIONS OF THE MODEL

5.5.1 BANK SOLUTION

Recall that the bank profile of the optimal stable channel is obtained when the water margin is reached and the two boundary conditions there are satisfied; (1) $D^* = 0$ and (2) $dD^*/dy^* = -\mu$. Whenever the value of dD^*/dy^* at a grid point is approximately equal to $-\mu$, the corresponding value of D^* is checked. If the value of D^* at that grid point is approximately equal to zero, then the water margin has been reached. However, the numerical scheme is such that D^* never really gets to zero. Thus, a criterion had to be established whereby the scheme is made to terminate when the value of D^* reaches some small but specified value; say 0.01. This means that when the depth at a grid point is 1% of the center channel depth, that point is considered to be at the water margin. The problem with using this criterion is that it causes the scheme to yield a value for B_s^* that is smaller than it should be, since the numerical scheme is made to terminate sooner than it should (at a depth that is not yet equal to zero). The stress-depth distribution over the channel boundary is also affected since it only covers the channel width determined by the numerical scheme, and not the 'true' channel width. The stress-depth distribution ends at the water margins determined using the termination criterion, which means that stress-depth is set to zero at these points. In reality, the stress-depths at these points should be non-zero since they are at depths that are very shallow, but still not equal to zero. In fact, the stress-depth distribution

should extend laterally beyond these points to the 'true' water margins. Because of this, the numerical scheme calculates values of bank water discharge that are slightly smaller than they should be.

The other problem encountered is that the termination criterion cannot really be specified arbitrarily. A criterion which allows convergence for a certain set of conditions may not necessarily lead to a convergent solution for another set of conditions. It turns out that for a given case, there is a minimum value of D^* that can be specified which will ensure convergence of the scheme. Fortunately, there is a way of determining this minimum D^* value. Examination of the expressions for ψ and $d\psi/dy^*$ in Equation 2 shows that the term '$2A_4 - {}^{17}/_3$' is found in the denominator. Therefore, the following condition must be satisfied in order to prevent 'divide by zero' errors from happening:

$$2A_4 - \tfrac{17}{3} \neq 0 \tag{54}$$

Using the definitions of A_4 and A_3 found after Equation 2, Equation 54 becomes

$$2\ln\left(\frac{30D^*\left(\frac{dD^{*2}}{dy^*}+1\right)^{0.5}}{\left(\frac{d_{90}}{D_c}\right)}\right)-\frac{17}{3}\neq 0 \tag{55}$$

At the water margin, $dD^*/dy^* = -\mu$. Plugging this in Equation 55 and rearranging yields the expression for the D^* value that will cause a 'divide by zero' error at the water margin.

$$D^* \neq \frac{d_{90}}{1.765\left(m^2+1\right)^{0.5}D_c} \tag{56}$$

Observation of the numerical model's behavior shows that specifying a value of D^* at the water margin that is smaller than that given by Equation 56 prevents the scheme from converging. Thus, in order to ensure that the scheme converges, one must specify a D^* value which satisfies the equation

$$D^* > \frac{d_{90}}{1.765\left(m^2+1\right)^{0.5}D_c} \tag{57}$$

For example, if $\mu = 0.84$, $d_{90} = 0.075$ m, and $D_c = 3.1$ m, Equation 57 yields $D^* > 0.0105$. This means that the scheme can only get as close as $0.0105D_c$ below the water surface; specifying a termination depth less than this would result in the scheme going on indefinitely.

Figure 5.20 shows the relation between the termination depth and the resulting value of B_s^*. The plot indicates that as the termination depth decreases, the value of B_s^* increases. Moreover, the plot can be approximated by a straight line which, when extrapolated, yields a B_s^* corresponding to zero termination depth. This would be a good estimate of the true value of B_s^*.

Even now that the true value of B_s^* is known, it is still necessary to determine D^*, dD^*/dy^*, d^2D^*/dy^{*2}, and d^3D^*/dy^{*3} from the point where the numerical scheme stops to the 'true' water margin. These values are needed to generate the stress-depth distribution over the channel's

true width. Since this portion of the boundary covers a relatively short distance, it can be estimated by a straight line. This will allow for a better approximation of the true stress-depth distribution, and consequently, the water discharge. However, it was again found that as long as the termination depth is less than $0.02D_c$, the difference in the water discharge will not really be significant. Thus the results of the numerical scheme are still adequate.

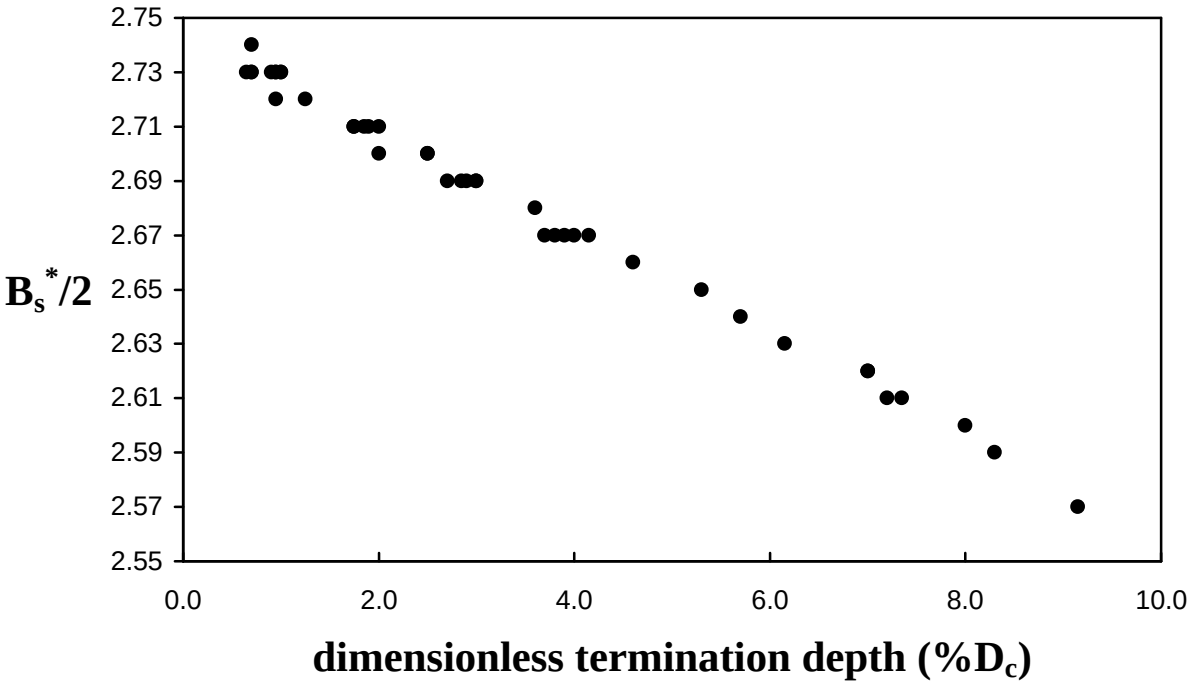

Figure 5.20. Relation between termination depth and resulting value of B_s^*

5.5.2 BED SOLUTION

Once the bank solution has been achieved, the values of D^*, dD^*/dy^*, d^2D^*/dy^{*2}, and $d\delta^*/dy^*$ on the bank side of the junction point will have been determined as well. These are used to calculate the lateral momentum flux, $\psi D^{*2}\{(dD^*/dy^*)^2+1\}(d\delta^*/dy^*)$, at that point. Since lateral momentum flux is continuous at the junction point, and ψ, D^*, and dD^*/dy^* on the bed side of the junction point are known, the value of $d\delta^*/dy^*$ on that side of the junction point can be determined. Plugging this value, as well as that of d_{cr}^*, in Equation 17, the flat-bed width B_f^* of the channel is calculated. Note that it is necessary for the value of 'm' in Equation 17 to be less than 1.0, but greater than or equal to zero, in order to get a physically meaningful solution (as 'm' approaches 1.0, B_f^* approaches infinity). It is this restriction which actually dictates the upper limit of the valid d_{cr}^* range for a given value of μ, $d_{cr\max}^*$.

It was observed that for a given μ value, as d_{cr}^* is increased, B_f^* also increases. As long as the value of 'm' is clearly less than 1.0, there should be no problems with the scheme

converging, i.e., yielding a value for B_f^*. At some point, however, it was found that minute increases in the value of d_{cr}^* resulted in drastic increases in B_f^*. This occurs when the value of 'm' approaches 1.0. The value of d_{cr}^* at which this starts to happen marks the transition from narrow to wide channels, and the corresponding B_f^* is the minimum dimensionless flat-bed width that a channel must have in order to be considered wide. The problem is that it is very difficult to define exactly what value of B_f^* separates narrow and wide channels, and the exact value of d_{cr}^* at which this occurs, because of the asymptotic nature of Equation 17.

As a result, the B_f^* value had to be estimated by visual inspection of plots of B_f^* vs. d_{cr}^*, for different values of μ (Figures 5.6a to 5.6g). It was decided that 5.0 would be an appropriate B_f^* value for all cases. Figures 5.6a to 5.6g show that below a B_f^* value of 5.0, the variation of B_f^* with d_{cr}^* is reasonably gradual while above it, the variation becomes so dramatic that the curves are practically vertical. This value of B_f^* can therefore be considered a good transition point from narrow to wide channels.

These figures also show that, although B_f^* still varies with d_{cr}^* for wide channels, the d_{cr}^* range over which this variation occurs is very small. Thus, for all practical purposes, wide channels can be thought of as existing at a single d_{cr}^* value for a given value of μ; that value being $d_{cr\max}^*$. Thus, Figures 5.6a to 5.6g can also be used to reasonably estimate $d_{cr\max}^*$ for different values of μ.

5.5.3 COMPOSITE SOLUTION

Once B_f^* has been determined, the flat-bed and bank regions are put together to obtain the complete channel profile. The stress-depth distribution for the entire channel is then determined by solving Equation 2 from the center of the channel to the water margin. A modified Dirac-delta function is used over a tiny region on the flat bed adjacent to the junction point, to account for the geometric discontinuities there.

The main problem for this phase of the numerical model is that a convergent solution can only be obtained up to a certain value of B_f^*. When the B_f^* value is greater than 35.0, the numerical scheme no longer terminates by itself. A possible explanation for this behavior is that the region over which the numerical scheme proceeds has become too long. As the scheme marches from one grid point to the next, tiny errors are generated with each step. These errors accumulate, and by the time the water margin is reached, the accumulated error has become too large for the boundary condition at the water margin ($\delta^* = 0$) to be satisfied. The width that is traversed has become so great that adjusting the starting value of δ^* (at the center of the channel) or changing the step size of the scheme no longer helps; the error at the water margin remains above what is considered tolerable.

However, it must be recalled that the stress-depth distribution of the entire channel can be obtained simply by combining the stress-depth distributions obtained from the bank and bed

solutions. The only reason Equation 2 is solved numerically from the center of the channel to the water margin is to make sure that the composite solution is correct. In each of the numerous numerical simulations that converged, the composite stresss-depth distribution and the stress-depth distribution used to verify it coincided. This strongly indicates that the composite stress-depth distribution resulting from the numerical model is correct, and that there is no longer a need to verify it in future runs.